

**THIS IS THE PEER REVIEWED VERSION OF
THE FOLLOWING ARTICLE:**

V. Volpe D. Davino L. Sorrentino G. Gorrasi R. Pantani
"SMART BEHAVIOR OF ELASTOMERIC COMPOSITES PRODUCED BY INJECTION MOLDING"
Journal of Applied Polymer Science
Volume 135, Issue 44, 20 November 2018, Article number 46863
DOI: 10.1002/app.46863

WHICH HAS BEEN PUBLISHED IN FINAL FORM AT
<https://onlinelibrary.wiley.com/doi/abs/10.1002/app.46863>

THIS ARTICLE MAY BE USED ONLY FOR NON-COMMERCIAL PURPOSES

Smart behavior of elastomeric composites produced by injection molding

Valentina Volpe^a, Daniele Davino^b, Luigi Sorrentino^c, Giuliana Gorrasi^a, Roberto Pantani^{a*}

^a*Department of Industrial Engineering, University of Salerno, Via Giovanni Paolo II, 132, 84084 Fisciano (SA), Italy*

^b*Department of Engineering, University of Sannio, Piazza Roma, 82100 Benevento, Italy*

^c*Institute of Polymers, Composites and Biomaterials (IPCB - CNR) Piazzale E. Fermi 1, 80055 Portici (Na), Italy*

* Corresponding author. Department of Industrial Engineering, University of Salerno, via Giovanni Paolo II 132, Fisciano, Salerno, Italy.

E-mail address: rpantani@unisa.it

ABSTRACT

This work reports the preparation and characterization of composites based on EVA and iron based powder produced by an injection molding machine specifically designed to host an electromagnet connected to a power supply which generates a magnetic field during the forming phases. The magnetic field allows the repositioning of the particles along the magnetic field lines leading to an anisotropic structural reinforcement. Thermogravimetric analyses show that the addition of iron powder to the EVA allows thermal stabilization, delaying the first degradation step ascribed to the loss of acetic acid. Mechanical characterizations show that the samples present a higher tensile modulus in the direction of the magnetic field with respect to the same property measured in the direction perpendicular to the magnetic field and considerably higher than the modulus of the samples obtained without the application of magnetic field. Furthermore, the samples obtained in the presence of magnetic field present a sensitivity to the application of an external magnetic field. These results demonstrate that the application of a magnetic field during the injection molding process of EVA/Fe composite induced an alignment of the particles, which therefore induce peculiar properties to the samples.

Keywords: Injection molding, magnetic field, EVA, Ferrite, mechanical characterization

1. Introduction

Polymeric composites can combine both the properties of the polymer matrix and the functional filler resulting in novel materials for designed applications tuning a polymer matrix property by introducing the appropriate filler that can respond to an external stimulus ^{1,2}. The use of magnetic fields, as external stimulus, is attracting great interest for several advantages. Generally, polymeric materials are not sensitive to magnetic stimuli. In order to produce a response to a magnetic field, the host matrix can be loaded with magnetic nanoparticles and show peculiar properties when exposed to static or alternating magnetic fields. The interaction between the magnetic moments of the particles and the magnetic field gradient can induce magneto-mechanical forces, which may be employed to change the shape of the host materials or to move the considered material. This approach can be utilized in several applications, like magnetic separation, actuators or drug delivery ^{3,4}. Moreover, magnetic nanoparticles can be employed as nano-heaters when exposed to an alternating magnetic field. Ethylene vinyl acetate (EVA) is a commodity copolymer of ethylene and vinyl acetate, with the vinyl acetate content typically ranging between 10 and 40 wt%. There are two types of chain segments in EVA: elastic and transition segments ⁵. Elastic segments confer elasticity to the manufacture in using conditions below the melting, while transition segments have the ability to reversibly change their stiffness from very soft and quasi-plastic at high temperatures to hard at low temperatures.

As it is a very important member of the family of engineering polymers, its physical and thermomechanical properties have been studied extensively and are well documented ⁶⁻⁸. Since EVA is also biocompatible and has been used in many biomedical engineering applications, such as in drug delivery devices ^{9,10} and its composites are often employed in the field of shape memory materials, like in heat-shrinking packaging ¹¹⁻¹⁴. In this optic it is very important to produce EVA based composites stimuli responsive. This paper reports the preparation and characterization of composites based on EVA and carbonyl iron powder using injection molding technology,

specifically designed to house an electromagnet connected to a power supply which generates a magnetic field during the filling phase. The magnetic field allows the repositioning of the particles along magnetic field lines leading to an anisotropic structural reinforcement. This alignment induces modulable properties to the obtained samples.

2. Experimental

2.1 Materials

The material adopted in this work is ethylene vinyl acetate (EVA) grade 1040VN4 supplied by Total (Courbevoie, France), a copolymer made by the high pressure polymerization process adding the comonomer (vinyl acetate – VA) in the main polymer chain based on ethylene monomer. Table 1 reports the properties of this material.

Table 1

Properties of EVA 1040VN4.

Property	Method	Unit	Typical value
Melt Flow Index (190°C/2.16 kg)	ISO 1133	g/10 min	4.5
VA content	Total Petrochemicals	%	14
Melt Temperature	ISO 11357	°C	90
Vicat Temperature	ISO 306	°C	68
Elasticity Modulus	ISO 527-2	MPa	62
Density	ISO 1183	g/cm ³	0.935

The magnetoparticles adopted in this work are Carbonyl Iron Powder produced by Sigma-Aldrich (Merck KGaA, Darmstadt, Germany). A masterbatch with 10% by volume of iron microparticles was produced with EVA by means of a twin screw extruder. Subsequently, the masterbatch was diluted with neat polymer directly in the injection molding machine (a 70ton CANBIMAT 65/185, from Negri-Bossi SpA, Italy) in order to obtain a compound with 1% and 2% by volume of iron

particles.

2.2 Injection molding

In this work, a 70-ton Negri-Bossi injection molding machine (CANBIMAT 65/185, from Negri-Bossi SpA, Italy) with a screw diameter of 25 mm and $L/D=22$ was used. An aluminum mold, in order to avoid interference with the magnetic field, was expressly designed to host an electromagnet which generates a magnetic field in the cavity (Fig. 1).

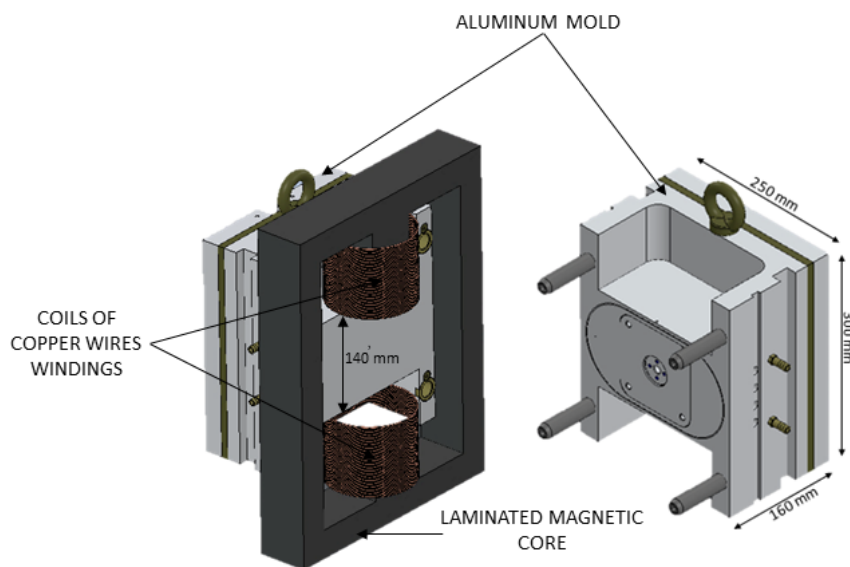


Fig. 1. Sketch of the Aluminum mold with the custom electromagnet.

The electromagnet is fixed to the stationary platen of the injection molding machine and consists of two coils of copper wires windings (copper wire diameter 1.4 mm, tolerance 2 mm, winding resistance is 6.7 Ohm) connected to a power supply (EA-PSI 8360-10 T) and a laminated magnetic core (iron sheets standard M300-35A ISO) to form an “iron circuit” for the magnetic field lines.

The number of spires and the geometry of the magnetic core allow to obtain a magnetic flux of 1.3 mWb.

The cavity geometry is shown in Fig. 2.

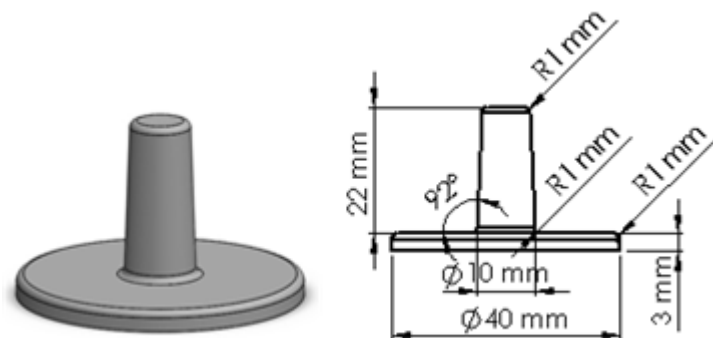


Fig. 2. Cavity geometry.

Table 2 reports the processing conditions adopted for the production of these samples.

Table 2

Processing condition for injection molding.

Temperature profile [°C] (increasing distance from the hopper to the nozzle)	180 - 190 - 200 - 200
Mold temperature [°C]	25 - 45
Filling pressure (hydraulic system) [bar]	80
Screw rotation speed [rpm]	120
Back pressure (hydraulic system) [bar]	2
Injection speed [%]	20
Shot size [cm ³]	6.4
Cooling time [s]	60
Iron content [% by volume]	1 - 2
Working current [A]	8 - 9
Working voltage [V]	115 - 120
Magnetic field "ON" time [s]	5

At the beginning of the injection phase during the injection molding process, the power supply is switched on so that the desired magnetic field is generated. The magnetic field is kept active for 5 seconds, in order to allow the orientation of the iron particles within the molten polymer.

3. Materials and Methods

3.1 X-ray diffraction (XRD)

XRD patterns were taken, in reflection, with an automatic Bruker diffractometer (equipped with a continuous scan attachment and a proportional counter), using nickel-filtered Cu K α radiation ($K\alpha = 1.54050 \text{ \AA}$) and operating at 40 kV and 40 mA, step scan 0.05° of 2θ and 3 s of counting time.

106 3.2 Rheology

107 A rheological characterization of the neat EVA and of the masterbatch was carried out by a Haake
108 Mars II (Thermo Haake GmbH, Germany) rotational rheometer in an oscillatory dynamic mode
109 with parallel plates configuration. The experiments were carried out at different temperatures (160
110 °C, 180 °C and 200 °C) thus obtaining the dependence of the complex viscosity on the oscillation
111 frequency. Master curves were then built at the temperature of 180 °C

112 3.3 SEM

113 The morphology of surface of the samples was analyzed by using a field emission scanning electron
114 microscope (FESEM, Zeiss SIGMA). The images were acquired by registering secondary electrons
115 with an Everhart-Thornley type detector.

116 3.4 TGA

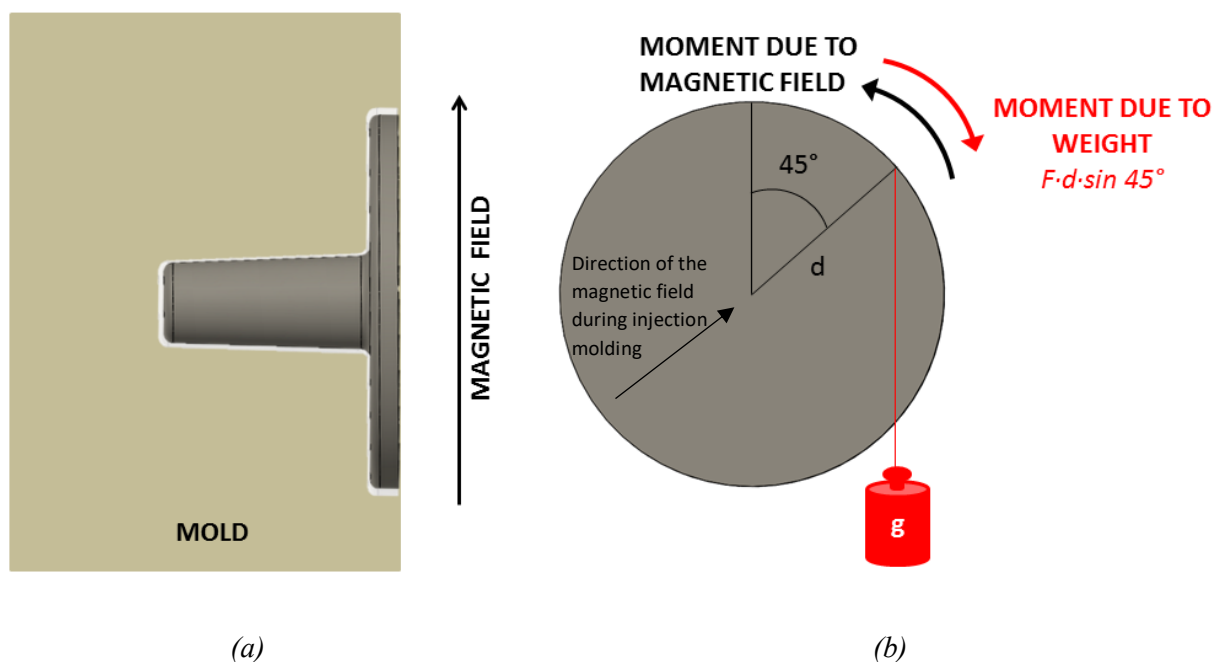
117 The analysis thermal stability of the samples was carried out by a TGA/DSTA 851 Mettler thermo-
118 balance with a nitrogen flow in order to create an inert atmosphere. The mass of each sample was
119 7–9 mg. The thermogravimetric curves were recorded in the course of heating from 25°C to 600°C
120 at a rate of 10°C/min.

121 3.5 Mechanical properties

122 Tensile properties were tested by using a Dual Column Tabletop Testing Systems (INSTRON,
123 series 5967) set with a cross head speed of 10 mm/min. The corresponding force was measured by a
124 30 kN machine load cell and converted to axial stress, whereas mechanical strain was calculated as
125 the machine crosshead displacement normalized by the gage length of the test specimen.

126 3.6 Assessment of magnetosensitivity

127 In order to quantify the maximum force that the sample performs to rotate and align the particles
128 oriented inside it with the magnetic field lines, a series of experiments were performed by
129 positioning the sample inside the cavity in which it was solidified and applying the magnetic field.
130 (Fig. 3a) The sample cannot translate because of the presence of the longer cylindrical part, but it
131 can rotate.



132 **Fig. 3.** Setup for measuring the sensitivity to magnetic field. a) side view of the position of the sample inside
 133 the moving half of the cavity. b) side view of the same sample, with a scheme of the counterweight used to
 134 measure the momentum induced by the presence of the magnetic field.

135

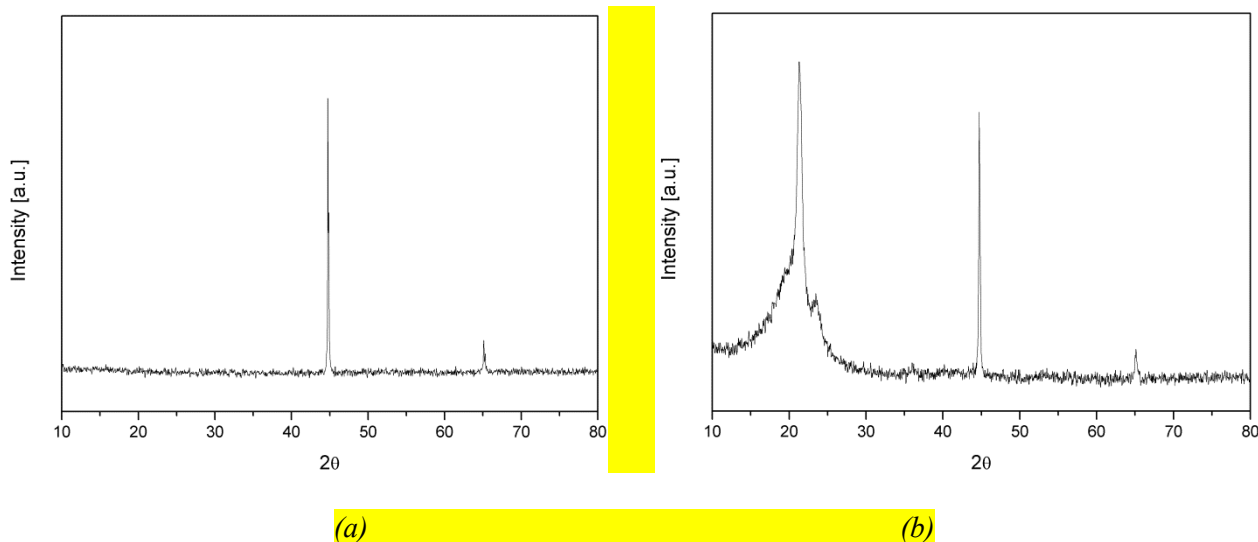
136 The sample was rotated 45 degrees with respect to the position in which it was formed (namely the
 137 direction of the magnetic field lines during injection molding). A lubricant was applied to minimize
 138 friction. In this configuration, by applying the magnetic field, the sample tends to rotate in order to
 139 recover its initial position, which assures an alignment of the oriented structures in the direction of
 140 the magnetic field. Increasing weights were then hanged by means of a wire connected at $d=19$ mm
 141 from the axis of the sample (fig. 3b), until the weight able to avoid the rotation was found. The
 142 moment of the force due to the weight represents in this configuration the moment due to the
 143 magnetic field and thus quantifies the sensitivity of the sample to the magnetic field itself.

144

145 4. Results and discussion

146 Figure 4 reports the XRD spectrum of the used filler and of the EVA/Fe masterbatch. For the
 147 Carbonyl Iron Powder two peaks at $2\theta=44.8^\circ$ and 65.2° are representative of the α -Fe (ferrite) and

148 related to the (1 1 0) and (2 0 0) reflections respectively, and a peak at 44.8° related to the (1 1 1)
 149 reflection of $\gamma\text{-Fe}$ ¹⁵. In addition to the representative peaks of the filler, the masterbatch presents two
 150 peaks at $2\theta=21.3^\circ$ and 22.8° , which were attributed to (110) and (200) characteristic crystal planes
 151 of polyethylene domain in EVA¹⁶.



154 **Fig. 4. XRD of Carbonyl Iron Powder (a) and masterbatch EVA/Iron (b)**

155 The flow curve at 180°C of the neat EVA adopted for this work is reported in Fig. 5. It can be
 156 noticed that the material presents the usual shear thinning behavior of thermoplastic polymers, and a
 157 relatively low viscosity at high shear rates. This rheological property is very important to allow the
 158 generation of aligned structures by effect of the magnetic field.

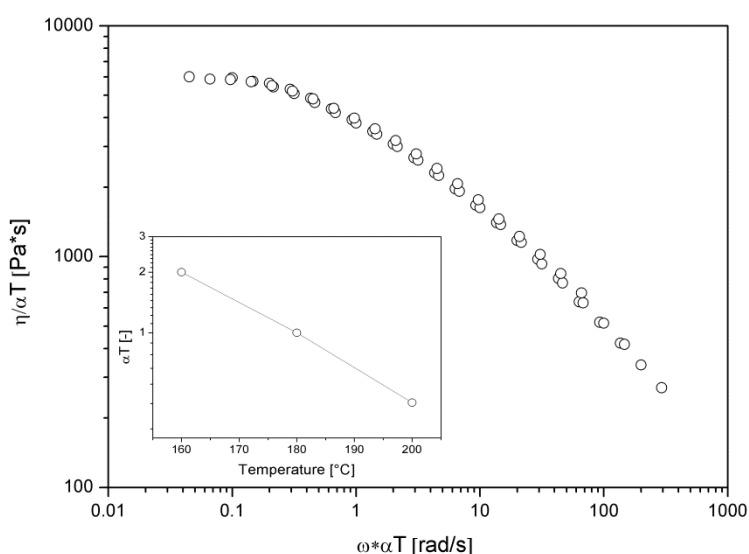


Fig. 5. Rheological properties neat EVA. Master curves at 180°C. The insert represents the shift factors describing the effect of temperature on viscosity

Thermogravimetric analysis (TGA) was carried out on neat EVA, masterbatch of EVA with Fe at 10% by volume and molded EVA reinforced with iron at 1% and 2% by volume. The TGA plots, reported in Fig. 6, show a residual mass zero in the neat EVA and increasing with the percentage of iron powder, up to a percentage in residual mass of 46.5% in case of EVA+Fe10% by volume. The residual mass content doesn't match exactly the Fe weight percent, and tends to increase with increasing the temperature. This could be due to the formation of iron oxides during the thermal scan, inducted by presence of traces oxygen in the oven and/or inside the EVA samples¹⁷.

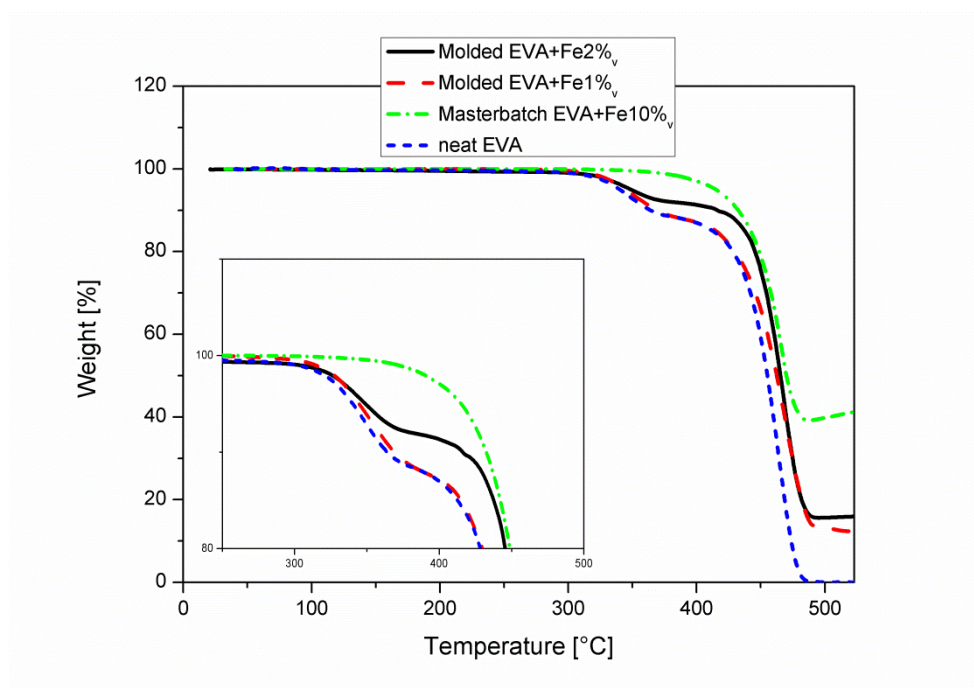
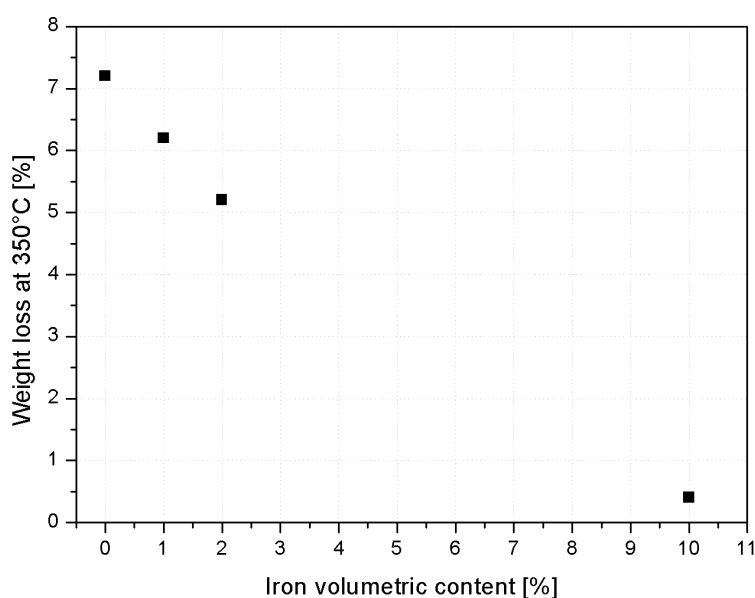


Fig. 6. Thermogravimetric analysis on neat EVA, masterbatch of EVA with Fe at 10% by volume and molded EVA reinforced with iron at 1% and 2% by volume.

The thermo-oxidation of EVA occurs in two steps¹⁸. Between 300 and 400°C deacetylation process is observed, with production of gaseous acetic acid and formation of double bonds carbon-carbon

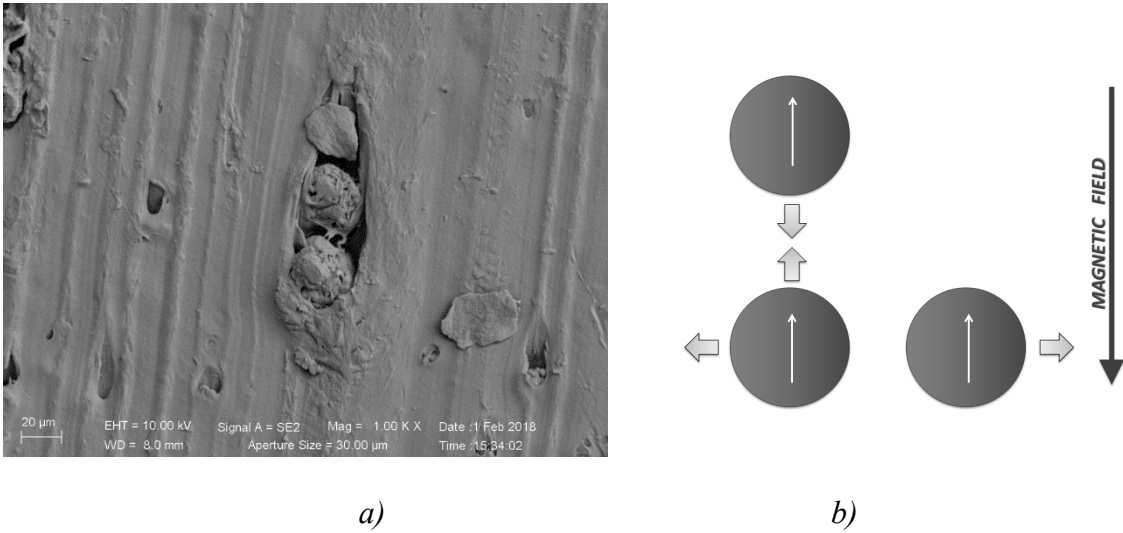
177 along the polymer backbone. In a second step, between 400 and 500 °C, the unsaturated chains are
 178 oxidized and volatilized through statistical chain breaking ¹⁹⁻²¹. By observing the magnification of
 179 the first weight loss in Fig. 6 it is possible to note a decreasing weight loss as the percentage of iron
 180 inside the polymer matrix increases. In fact, the iron powder acts as thermal stabilizer, decreasing or
 181 preventing the emission of acetic acid inside the EVA. By observing, for all the analyzed
 182 composites, the weight loss at 350°C (Fig. 7), temperature at which the emission of acetic acid
 183 should have already occurred, it is possible to note as at increasing iron volumetric percentage the
 184 weight loss almost linearly decreases.



185
 186 **Fig. 7.** Weight loss at 350°C corresponding to the mixtures containing different iron volumetric percentages.

187
 188 The presence of a magnetic field during the injection phase of the molding process involves a
 189 rearrangement of the particles, which move themselves by developing chain-like structures that
 190 aligning according to the magnetic field lines. In Fig. 8a it is possible to observe a SEM
 191 micrographs showing a particles alignment in a sample of EVA+Fe 2% by volume. The scheme of
 192 the interaction between magnetic particles in presence of magnetic field is shown in Fig. 8b and
 193 illustrates the reason of the build-up of chain like.

194



195

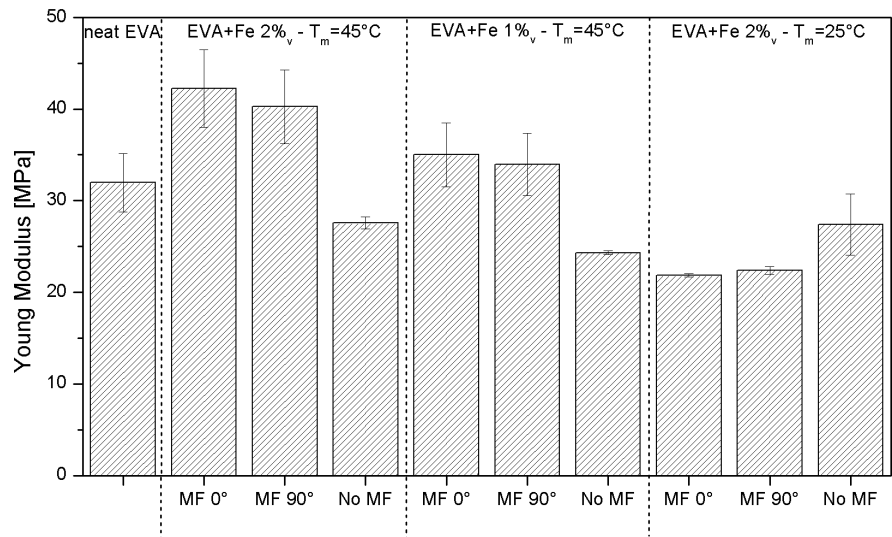
196

197 **Fig. 8.** a) SEM micrographs showing a particles alignment in a sample of EVA+Fe 2% by volume; b)
198 Interaction scheme of magnetic particles.

199

200 The alignment of the particles to the magnetic field lines is strongly connected to the temperature
201 profile in the cavity. Since the solidification proceeds from the sample surface toward the core, the
202 external layers quickly reach a high viscosity, whereby the action of the magnetic field is not
203 sufficient to impart an orientation. For this reason, in the external layers the particles are distributed
204 without a particular order, while in core layer an alignment of particles to the magnetic field lines
205 can be observed ²². This peculiar distribution of particles, due to the presence of a magnetic field,
206 leads to an anisotropic structural reinforcement to the molded part, which can be dependent not only
207 on the applied magnetic field, but also on the percentage of iron inside the elastomeric matrix and
208 the mold temperature. In order to quantify this structural reinforcement, the mechanical properties
209 of the samples were characterized in tension mode. Fig. 9 shows the Young modulus (MPa) of the
210 molded parts of neat EVA, EVA filled with iron particles at 2% by volume obtained with mold
211 temperature (T_m) at 25°C and 45°C, and EVA with iron particles at 1% by volume obtained with
212 mold temperature at 45°C. For each condition, the sample obtained without magnetic field (“No
213 MF”), which presents a random arrangement of the particles, was compared with the samples

214 obtained in the presence of magnetic field, tested both in the direction parallel to the alignment
 215 direction of the particles (“MF 0°”) and in the perpendicular direction (“MF 90°”).



216
 217 **Fig. 9.** Young’s modulus of the samples of neat EVA, EVA+Fe 2%v with mold temperature 25°C and 45°C
 218 and EVA+Fe 1%v with mold temperature 45°C. Comparison between the samples molded without magnetic
 219 field (“No MF”) and the samples tested in the direction parallel (“MF 0°”) and perpendicular (“MF 90°”) to
 220 the alignment direction of the particles.

221
 222 Results obtained in terms of Young modulus showed that, without magnetic field, adding iron
 223 powder to the elastomeric matrix does not influence the mechanical properties of the EVA. On the
 224 contrary, in the presence of magnetic field the Young modulus increases considerably. In particular,
 225 for each condition, the samples in which the particles are oriented in the same direction of the
 226 magnetic field lines (MF 0°) present a Young modulus considerably higher than that of the
 227 corresponding sample with randomly dispersed particles. The Young modulus of the samples in
 228 which the particles are oriented in the perpendicular direction with respect to the magnetic field
 229 lines (MF 90°), also larger than the corresponding sample with randomly dispersed particles, is
 230 slightly lower than that of the sample with particles oriented in the same direction of the field lines
 231 (MF 0°). These results demonstrate that the application of a magnetic field during the injection

232 process of EVA/Fe composites favors an anisotropic reinforcement to the molded part, which is
233 more effective if the iron particles are aligned in the same direction of the magnetic field. This
234 effect is more evident for higher percentages of iron powder inside the composite. Furthermore,
235 from mechanical tests it was possible to deduce that the mold temperature has a significant effect on
236 such properties: at lower mold temperatures it is not possible to observe the effect of the magnetic
237 field. In fact, a higher mold wall temperature induces a slower cooling rate of the melt which
238 remains for a longer time at low enough viscosity values to allow the movement of the particles and
239 thus an alignment according to the magnetic field lines. On the contrary, a low mold wall
240 temperature results in a higher cooling rate, so the difficult of the particles to move in a more
241 viscous matrix involves in an almost random iron distribution.

242 The presence of chain-like structures aligned to the magnetic field lines can also be detected by
243 placing the molded sample, free to move, inside a magnetic field (Fig. 10). In fact, when the
244 magnetic field is activated, the sample instantly responds by rotating in order to align the chain-like
245 structures to the applied magnetic field lines. The position taken by the sample, free to move, under
246 a magnetic field indirectly confirms the effect of the magnetic field on iron particles in the
247 elastomeric matrix during the injection phase. In Fig. 10 it is possible to observe the sample
248 positioned under the magnetic field, free to move: in Fig. 10a the magnetic field is off; in Fig. 10b
249 the magnetic field is on and the sample rotates to align the orientation inside it with the magnetic
250 field lines. The images shown in Fig 10 have been extracted from a video filmed during the
251 experiment described in paragraph 3.6.

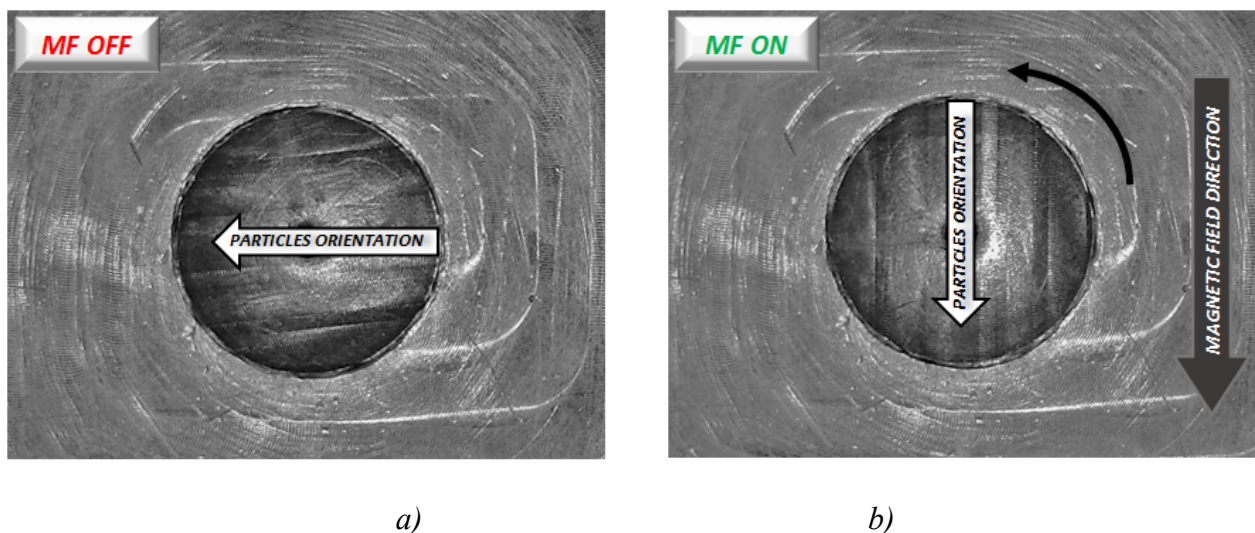


Fig. 10. EVA+Fe 2%v sample positioned under the magnetic field free to: a) MF OFF; b) MF ON.

The momentum induced by the magnetic field, which causes the rotation, was measured with the method schematized in Fig. 3. It was found that for a weight fraction of 1% the momentum was measured as $4.2 \cdot 10^{-4} \pm 7 \cdot 10^{-5} \text{ N}\cdot\text{m}$, whereas for a weight fraction of 2% the momentum was measured as $9.8 \cdot 10^{-4} \pm 5 \cdot 10^{-5} \text{ N}\cdot\text{m}$. The momentum results thus increasing with the percentage of iron, as expected, and the increase is consistent with a linear dependence upon the filler content. Furthermore, the samples show a sensitivity to the application of a magnetic field. In particular, they tend to align the direction of the pristine magnetic field (namely the direction of the field lines during the forming process) in the direction of the applied external magnetic field. The moment of the force which induces this rotation is consistent with a linear dependence upon the filler content.

This phenomenon could be exploited in devices for microfluidics, e. g. peristaltic micropumps with magnetic control.

5. Conclusions

In this work, the characterization of composites based on EVA and iron powder produced by injection molding was carried out. The addition of the iron powder to the EVA allows a thermal

272 stabilization, preserving the material from the premature decomposition due to the emission of
273 acetic acid. Furthermore, it was demonstrated that the application of a magnetic field in the mold
274 cavity during the injection phase of the injection molding process allows the repositioning of the
275 iron particles along magnetic field lines, leading to an anisotropic structural reinforcement. Such
276 reinforcement, demonstrated by tensile test of the composites, increases with the iron content in the
277 elastomeric matrix and with the mold temperature.

278

279 **Acknowledgements**

280 These research activities were supported by the Italian Ministry of Education and Research (MIUR)
281 within the PRIN project developing polymeric smart foams with behaviour controlled by the
282 magnetic field – E.PO.CA.M. (grant number PRIN 2012JWPMN9). The authors gratefully
283 acknowledge Antonio Vecchione and Rosalba Fittipaldi from CNR-SPIN and Dept. of Physics “E.
284 R. Caianiello”, University of Salerno, for their technical support in scanning electron microscopy
285 analysis.

286

287 **References**

288

- 289 1. Behrens, S., *Nanoscale* 3, 877 2011.
- 290 2. Wei, S. Y.; Patil, R.; Sun, L. Y.; Haldolaarachchige, N.; Chen, X. L.; Young, D. P.; Guo, Z. H., *Macromol*
291 *Mater Eng* 296, 850 2011.
- 292 3. Behrens, S.; Appel, I., *Curr Opin Biotech* 39, 89 2016.
- 293 4. Chertovich, A. V.; Stepanov, G. V.; Kramarenko, E. Y.; Khokhlov, A. R., *Macromol Mater Eng* 295, 336
294 2010.
- 295 5. Huang, W. M.; Zhao, Y.; Wang, C. C.; Ding, Z.; Purnawali, H.; Tang, C.; Zhang, J. L., *J Polym Res*
296 192012.
- 297 6. Bianchi, O.; Oliveira, R. V. B.; Fiorio, R.; Martins, J. D. N.; Zattera, A. J.; Canto, L. B., *Polym Test* 27,
298 722 2008.
- 299 7. Stelescu, M. D.; Manaila, E.; Craciun, G.; Zuga, N., *Polym Bull* 68, 263 2012.
- 300 8. Wu, X. L.; Huang, W. M.; Tan, H. X., *J Polym Res* 202013.
- 301 9. Arun, M.; Silja, P. K.; Mohanan, P. V., *Toxicol Mech Method* 21, 561 2011.
- 302 10. Matsumura, K.; Hyon, S. H.; Nakajima, N.; Peng, C.; Tsutsumi, S., *J Biomed Mater Res* 50, 512 2000.
- 303 11. Li, F. K.; Zhu, W.; Zhang, X.; Zhao, C. T.; Xu, M., *J Appl Polym Sci* 71, 1063 1999.
- 304 12. Mishra, J. K.; Das, C. K., *J Mater Sci Lett* 20, 1877 2001.
- 305 13. Tanrattanakul, V.; Kaewprakob, T., *J Appl Polym Sci* 112, 1817 2009.

- 306 14. Tanrattanakul, V.; Kaewprakob, T., J Appl Polym Sci 119, 38 2011.
307 15. Yang, J.; Lian, J.; Dong, Q.; Guo, Z., Appl Surf Sci 229, 2 2004.
308 16. Dubey, K. A.; Majji, S.; Sinha, S. K.; Bhardwaj, Y. K.; Acharya, S.; Chaudhari, C. V.; Varshney, L., Mater
309 Chem Phys 143, 149 2013.
310 17. Lysenko, E. N.; Surzhikov, A. P.; Zhuravkov, S. P.; Vlasov, V. A.; Pustovalov, A. V.; Yavorovsky, N. A.,
311 Journal of Thermal Analysis and Calorimetry 115, 1447 2014.
312 18. Riva, A.; Zanetti, M.; Braglia, M.; Camino, G.; Falqui, L., Polym Degrad Stabil 77, 299 2002.
313 19. Boguski, J.; Przybytniak, G.; Lyczko, K., Radiat Phys Chem 100, 49 2014.
314 20. Liu, C. P.; Wang, M. K.; Xie, J. C.; Zhang, W. X.; Tong, Q. S., Polym Degrad Stabil 98, 1963 2013.
315 21. Reyes-Labarta, J. A.; Olaya, M. M.; Marcilla, A., Polymer 47, 8194 2006.
316 22. Volpe, V.; D'Auria, M.; Sorrentino, L.; Davino, D.; Pantani, R., Materials Today Communications 15,
317 280 2018.

318